LETTERS

BEHAVIOUR OF METALLIC DROPLETS IN A TOKAMAK PLASMA

D. HILDEBRANDT, B. JÜTTNER, H. PURSCH
(Central Institute of Electron Physics, Academy of Sciences of the German Democratic Republic, Berlin);
K. JAKUBKA, J. STÖCKEL, F. ZACEK
(Institute of Plasma Physics, Czechoslovak Academy of Sciences, Prague)

ABSTRACT. Micrometre sized tantalum droplets were injected into a tokamak plasma by a controllable arcing gun located behind the wall. The trajectories of the ablating particles were photographed by a high speed camera. Various possible mechanisms which may explain the observed curvature of the particle paths are discussed. The migration of the ablated material in the tokamak was studied by post-mortem analysis of collector probes and limiters.

1. INTRODUCTION

In a tokamak, the energy and particle fluxes show spatial and temporal variations, which can be differently pronounced in the two toroidal directions. This may influence the trajectories of injected particles, for example pellets used for controlling the plasma density, and may cause a curved path [1]. The same holds for liquid metal droplets which are ejected from the inner surface as a result of plasma–wall interaction (surface melting, arcing [2]). These droplets can penetrate into the plasma where they become evaporated and contaminate the plasma. Thus, the stability of a discharge is influenced by the behaviour of the particles.

Since little is known about the fate of flying particles and their evaporation products in a tokamak, a special experiment has been performed in the tokamak Castor, using electric arcs as a source of liquid metal droplets. Before and during injection, the edge plasma and the impurity fluxes were studied by Langmuir and collector probes at various toroidal locations [3, 4].

2. EXPERIMENTAL DETAILS

2.1. The tokamak

Castor is a small tokamak with a major radius of 0.4 m, and minor radii of the first wall and limiters of 0.105 m and 0.075–0.085 m, respectively [3]. The limiting values are: plasma current I_p = 30 kA, pulse length t = 9 ms and toroidal field B_T = 2.0 T. The line averaged electron density can be varied in the range of (0.3–2.0) × 10^{19} m^{-3}, the central electron temperature amounts to 150–300 eV and the central ion temperature is 50–100 eV. Several toroidally distributed probes were used for measurements of the electron temperature, electron density, impurity fluxes and the impact energy of plasma ions on solid surfaces. Figure 1 shows schematically the locations of the limiters, the arcing gun, the probes and other diagnostic equipment.

2.2. The particle source

The advantage of applying electric arcs as particle sources consists in the simplicity of the device for all conducting materials and the easy control. With arc currents above 100 A, many droplets are ejected from the cathode [5]. Other erosion components are ions and neutral vapour. The ion erosion rate can become comparable with the rate of droplet ejection, which is about 10^{-4} $g \cdot C^{-1}$ [5] (with small cathodes and high currents the droplet rate may exceed 10^{-3} $g \cdot C^{-1}$ [5]). However, in a tokamak these metal ions cannot enter the inner plasma region because of the magnetic field. This is not true for neutral metal atoms, but the amount of neutral vapour leaving the cathode is smaller than the amount of ions by several orders of magnitude, as can be deduced from measurements with laser induced fluorescence [6]. So, only droplets

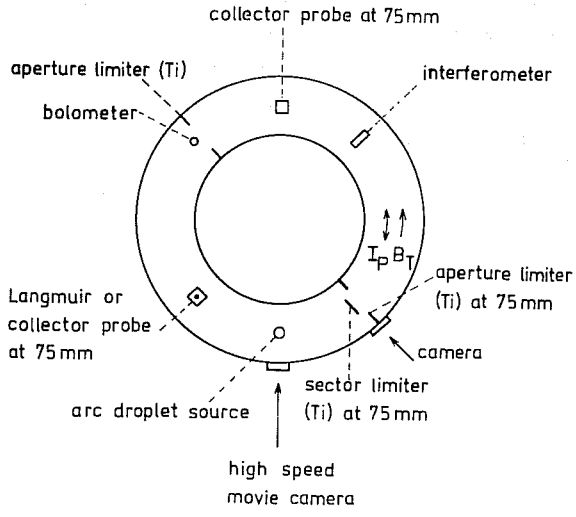

FIG. 1. Location of limiters, arc droplet source (arcing gun), probes and other diagnostics.

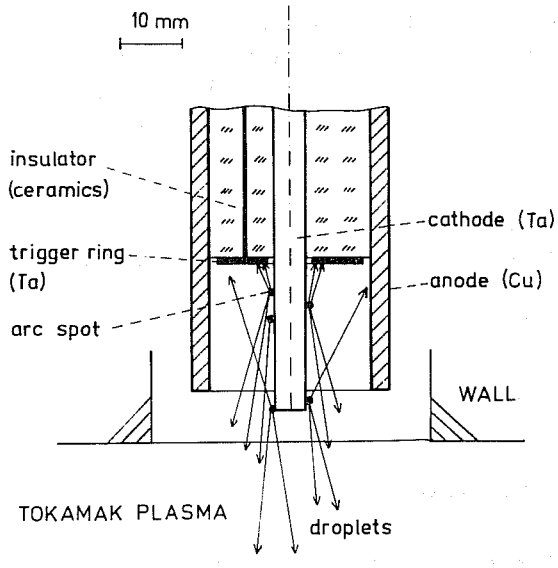

FIG. 2. Construction of the arcing gun.

remain as important erosion products which can enter the plasma. A disadvantage of arcing is the sometimes large variation in size of the droplets, whose diameter can range from 1 to 100 μm [7].

In the present experiment, tantalum was used as the material for injection because it constituted a non-intrinsic impurity. An arcing gun was positioned behind the wall at a minor radius of 0.115 m. It had a coaxial construction, with the tantalum cathode as the inner electrode (see Fig. 2). The arc was ignited by a spark between a trigger ring and the cathode in the interior of the gun. The discharge was fed by a capacitor; it had maximum currents of several kiloamperes and a duration of 1–3 ms. During this time the arc was driven to the tip of the cathode (towards the tokamak plasma). This movement prevented gross heating of the cathode. Melting occurred only within the cathode spots. From these spots, the particles were ejected at small angles to the cathode surface [5]. The gun was fired at a pre-selected instant of the tokamak discharge, mostly during the current plateau phase.

Tests in a separate vacuum system showed that the gun emitted droplets with a size of around 1 μm, and the amount of other matter emitted from the gun was reduced by two orders of magnitude when a magnetic field was applied; however, the droplet emission was not influenced and thus, except for the droplets, the ejected matter was highly ionized.

2.3. Experimental procedure

The parameters in the tokamak Castor were: plasma current I_p = 10 kA, line averaged electron density $n_e = (0.4–1) \times 10^{19}$ m^{-3}, toroidal magnetic field B_T = 1.35 T, safety factor q = 10 and discharge duration t = 9 ms. Generally, the plasma current was in the same direction as the toroidal magnetic field, but some experiments were carried out with the direction of I_p reversed. In the plateau phase of the plasma current, arcs were ignited in the arcing gun to emit metallic droplets into the plasma.

To minimize gas emission, the arcs in the arcing gun were conditioned in vacuum. The trajectories of the ejected droplets were recorded with a high speed movie camera running at 1000 frames per second. The collector probes for analysing the impurity fluxes and measuring the impact energies of the plasma ions could be retracted and positioned at various points of the minor radius; thus the effects of conditioning, injection and normal operation of the tokamak could be distinguished. After exposure, the samples and the limiters were replaced and analysed by Rutherford backscattering.

3. RESULTS AND DISCUSSION

The Langmuir probes yielded values for the electron density n_e and the electron temperature T_e at the plasma edge (minor radius 80–100 mm) in the range of $(1–6) \times 10^{18}$ m^{-3} and 10–40 eV, respectively [3]. For the plasma ions, impact energies of 60–150 eV could be deduced from the lattice damage [3] found on single crystal collectors. This agrees with the energy gained by particle acceleration in the Langmuir sheath around the probes (about 3 kT_e). These values showed remarkable differences in the ion and the electron drift directions; the values in the ion drift direction were larger inside the separatrix and smaller outside. Also the fluxes of the intrinsic impurities showed characteristic differences in the ion and the electron drift directions [3]. The toroidal flow of tantalum evaporated from injected droplets also indicated such differences [4].

The tokamak parameters, such as the loop voltage U_ℓ, the line averaged electron density n_e and the radiated power P_r, were affected by droplet injection, as shown in Fig. 3. The gun was fired in the plateau phase, 3 ms after starting the tokamak discharge. The time resolved photographs gave the number of injected particles within the core plasma as a function of time; this is shown in Fig. 4. Typically, the signals of U_ℓ and P_r exhibited two separate maxima. The first peak occurred immediately after arc ignition. This maximum may be caused partly by the release of matter from the cathode; an electric perturbation seems also possible

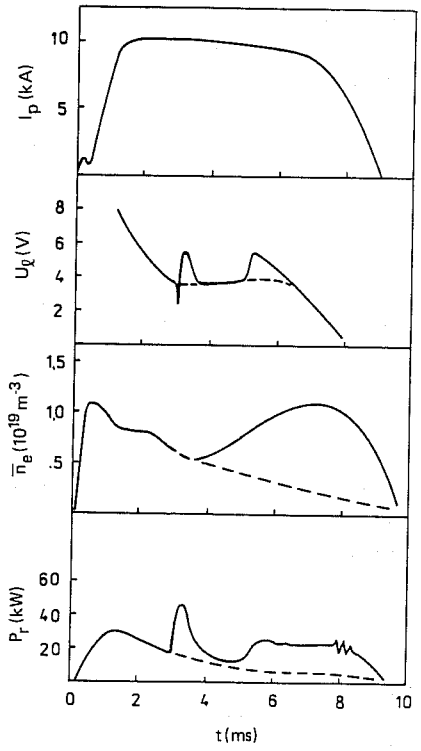

FIG. 3. Diagnostic traces of plasma current I_p, loop voltage U_ℓ, line averaged electron density n_e and radiated power P_r versus time for a discharge with strong injection at 3 ms. Dashed curves: without injection.

because almost no particles could be seen at that time. At the time of the second peak, however, about 2–3 ms later, there was a maximum number of particles within the plasma (see Fig. 4). The delay of the second peak has two reasons. First, a certain time is needed for the arc discharge to reach the tip of the cathode and, second, the droplets have a finite time of flight. Particle velocities of the order of about 100 m·s^{-1} were deduced from the photographs.

The flying droplets showed deflections only in the counter-direction to the plasma current, as can be seen in Figs 5 and 6. With the direction of the plasma current reversed, the deflection was toroidally opposite. The visible traces of particles with lower velocities were not simple continuous curves but showed an extension towards the bottom of the torus (arrows in Fig. 5). This can be explained by the electron drift in the toroidal magnetic field [4] and indicates that the trajectories become visible through the emission of light from the evaporating matter.

The deflection of the macroparticles started when the droplets entered the plasma and then continued (Fig. 5). Sometimes, there were sudden changes (Fig. 6), which were associated with a puff of metal vapour. Such local evaporation was also observed at the installed Langmuir probes (see Fig. 7). Of particular interest are the circular holes burnt into the surface. They were also found with highly degassed samples, which leads to the conclusion that they cannot be the result of gas pocket explosions.

Intrinsic dust particles removed from the wall and limiters in discharges without arc ignition showed strongly curved trajectories, which may be due to their low emission velocity (see Fig. 8). Hence the effect is general and is not due to plasma disturbances caused by arcing.

The observed deflections of the droplets released by arcing indicate an acceleration up to values of some 10^4 m·s^{-2}. The corresponding forces must be variable on a time-scale of milliseconds. The possible mechanisms for these processes are as follows:

(1) Charging of the droplets and deflection by electric fields;
(2) Momentum transfer by asymmetric impact of plasma ions;
(3) Repulsion by asymmetric ablation due to anisotropic heat fluxes (mainly by the plasma electrons) or to runaway electrons.

It is not possible that other plausible forces [8] (for example the effect of the toroidal magnetic field on the motion of charged droplets) deflect the particles in the counter-direction to the plasma current.

In case (1), we must consider the electric field caused by the loop voltage U_ℓ and the droplet charge q caused by the contact with the plasma. Then the acceleration a is

$$a = q \cdot U_\ell / 2\pi R \cdot M \qquad (1)$$

where R is the major radius and M is the particle mass. The charge q depends on the particle radius r_T and the electric field, $E = (4\pi n_e k T_e)^{1/2}$, in the Langmuir sheath, $q = 4\pi\epsilon_0 E r_T^2$.

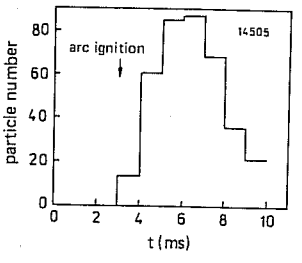

FIG. 4. Number of macroparticles ejected by arcing, as observed on the photographs at different times.

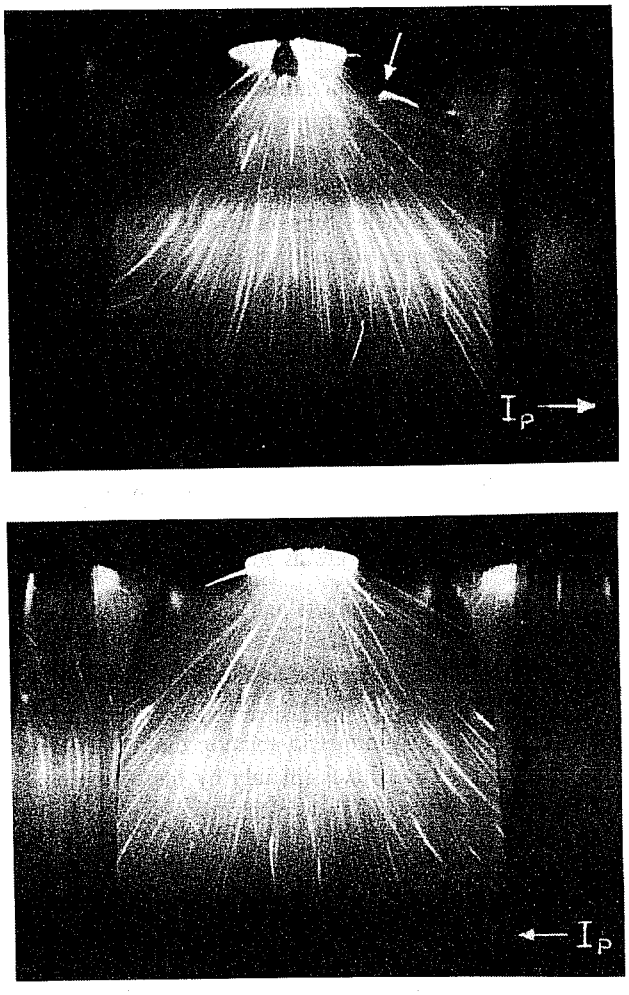

FIG. 5. Photographs taken at different orientations of the plasma current. The time elapsed after start of the tokamak discharge is 5 ms.

With $kT_e = 300$ eV, $n_e = 10^{19}$ m^{-3} and $U_f = 2.5$ V, the acceleration of tantalum particles is about $4 \times 10^{-8}/r_T$ (in SI units). With particle radii of $\simeq 1$ μm, the acceleration is 4×10^{-2} m·s^{-2}; this is much too small to explain the observed deflections. Hence collisional or repulsive forces must be taken into consideration.

Momentum can be transferred to macroparticles by the impinging plasma ions and by atomic particles emitted from the surface of the macroparticles owing to ion reflection, sputtering and ablation. Because of the lower electron mass, the direct contribution of electrons to momentum transfer is much smaller than that of ions, although the ions receive their energy mainly from the sheath which is maintained by the electron flow. To estimate the contributions of these particle fluxes to the momentum transfer to the macroparticles, the fractions of energy consumed by the different processes have to be considered.

Assuming first that only plasma ions carry energy to a macroparticle (case (2)) and that this has already a temperature at which sublimation occurs, the conservation of energy requires that

$$E_p = \gamma_r E_r + \gamma_s E_s + \gamma_a E_a + h_s (\gamma_s + \gamma_a) \qquad (2)$$

where $E_{p,r,s,a}$ are the mean energies of the incident and reflected plasma ions, and the sputtered and ablated tantalum atoms, respectively, $\gamma_{r,s,a}$ are the particle reflection coefficient, the sputtering yield of tantalum and the number of ablated tantalum atoms per incident ion, respectively, and h_s is the heat of sublimation. The fractions of energy of the impinging plasma ions consumed for reflection, sputtering and ablation, and hence the contribution of these processes to the momentum transfer to macroparticles depend on the impact energy of the protons.

Considering the ion acceleration by the sheath, the ion impact energy E_p is about 1 keV, with an ion temperature of 100 eV and an electron temperature of 300 eV in the core plasma. Typical values for particle reflection [9] are $\gamma_r = 0.2$ and $E_r = 0.5\ E_p$, and typical values for sputtering [10] are $\gamma_s = 10^{-3}$ and $E_s = 10$ eV. Corresponding to a sublimation temperature of about 3000 K, the energy of the ablated tantalum atoms is about 0.3 eV and h_s is 3 eV.

From these estimated values it can be concluded that about 90% of the ion impact energy is consumed for ablation and about 9% is converted into kinetic energy of the ablated atoms ($E_a/h_s = 0.1$). The number of ablated atoms per incident proton is about 300.

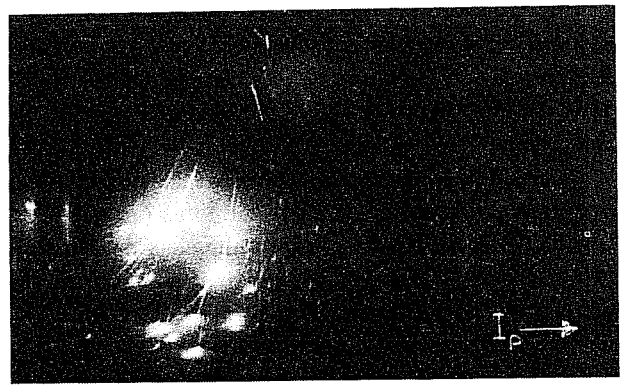

FIG. 6. Photograph showing sudden path deflections of macroparticles ejected by arcing and the ablated vapour clouds. Exposure time 1 ms.

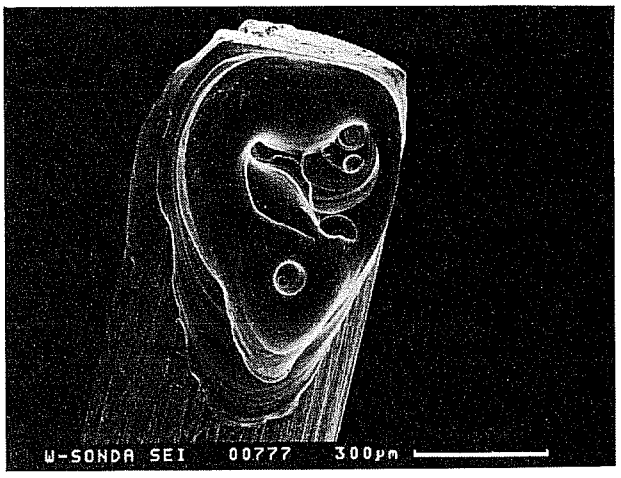

FIG. 7. Traces of local heating at a Langmuir probe.

The momentum transferred to a macroparticle per incident proton, Δp_M, expressed in terms of energy, is

$$\Delta p_M = (2E_p m_H)^{1/2} - \gamma_r (2E_r m_H)^{1/2} - \gamma_s (E_s m_{Ta})^{1/2} - \gamma_a (2E_a m_{Ta})^{1/2} \quad (3)$$

where m_H is the mass of a hydrogen atom and m_{Ta} is the mass of a tantalum atom. Inserting the values mentioned above, the relative contributions of the particle fluxes of primary and reflected protons, and of sputtered and ablated atoms to Δp_M are about 10^{-2}, 10^{-3}, 2×10^{-5} and 0.99, respectively.

This demonstrates that the deflection of the droplets must be due to anisotropic ablation, even if only atomic particle fluxes are taken into account. Hence the continuous deflection of macroparticles is an indication of a preferential heat flux in the counter-direction to the plasma current in the core plasma. For other tokamaks, such curved trajectories of injected pellets have also been reported [1].

The contribution of ablation to momentum transfer is even more dominant when the heat flux due to electrons is considered as well.

Most probably, the suprathermal electrons carry an anisotropic heat flux to the macroparticles, as suggested in Ref. [1], and therefore we favour case (3). The absolute value of the anisotropic heat flux Q can be estimated, taking into account that deflection can be observed when the momentum transferred to a macroparticle by the ablating atoms equals approximately the original momentum of the macroparticle $M \cdot v_0$. Hence,

$$M \cdot v_0 = \dot{N}\, \Delta t \cdot m_{Ta} v_a \quad (4)$$

where $\dot{N}$ is the ablation rate, Δt is the time-scale and $m_{Ta}v_a$ is the momentum of an ablated tantalum atom.

The ablation rate is obtained by $\dot{N} = 0.9\, Q \cdot A/h_s$, where A is the cross-section of the macroparticle. Hence,

$$Q = h_s \cdot M \cdot a/0.9 \cdot A \cdot m_{Ta} v_a \quad (5)$$

where $a = v_0/\Delta t$ is the particle acceleration.

With an observed acceleration of 10^4 m·s^{-2} and a particle size of 1 μm, we obtain $Q = 10^{18}$ eV·s^{-1}·mm^{-2}, which corresponds to an asymmetry of a few per cent of the heat flux estimated using the values of n_e and T_e in the core plasma.

A special effect can occur if runaway electrons impinge on a particle, causing instantaneous evaporation. The sudden path changes shown in Fig. 6 are probably associated with such events. The observed deflections occurred in a time-span shorter than 10^{-5} s. Assuming a particle size of 1 μm and a particle velocity of 100 m·s^{-1}, a heat flux Q of about 160 W·mm^{-2} has been found to be necessary for a deflection of macroparticles within 10^{-5} s. With this value of the heat flux, the circular holes burnt into the surface of the installed Langmuir probes can be explained by local pulse heating and evaporation due to runaway electron impact [11]. The electron energy required for a heat pulse with a duration of 10^{-5} s is about 10 keV, assuming a current density of 10^3 A·mm^{-2} and an energy efficiency of 0.1% [11]. The occurrence of electrons with energies higher than 10 keV in Castor

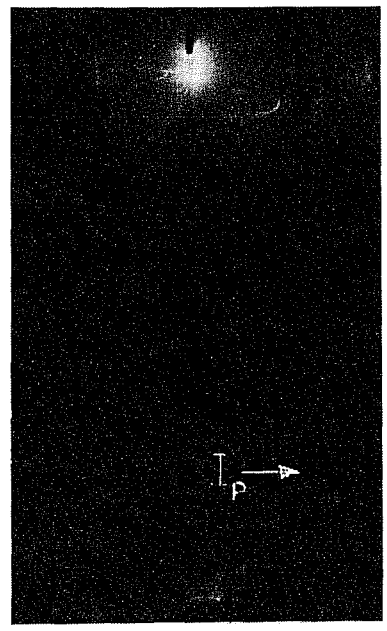

FIG. 8. Photograph of the plasma in the vicinity of the limiter, showing the path of dust particles released from the wall.

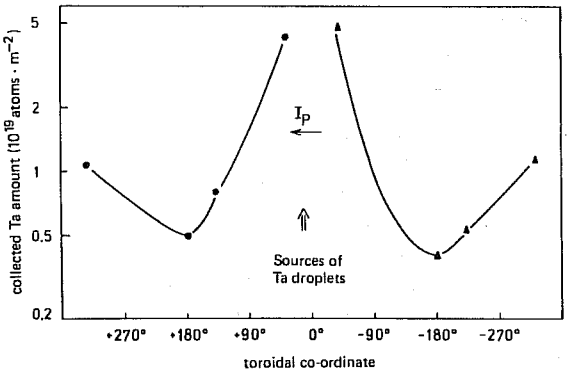

FIG. 9. Deposition of tantalum at a radial position of 80 mm as a function of the toroidal co-ordinate.
● — *surfaces facing the ion drift side,*
▲ — *surfaces facing the electron drift side.*

discharges is documented by the observation of hard X-ray emission.

Migration of the evaporated droplet material was studied by post-mortem surface analysis of different collector probes and limiter parts which were replaced after a series of experiments. A typical toroidal variation of the droplet material deposited on limiters and probes on the top side of the torus at a radial position of 80 mm is shown in Fig. 9 for surfaces facing the two toroidal directions (ion drift side and electron drift side). The injected material has a non-uniform distribution. The deposition rate is strongly peaked on the surfaces facing the particle source and is lowest on the surfaces 180° toroidally away from the source, the difference amounting to about one order of magnitude. While the deposition near the source is influenced by the emission properties of the source, the deposition on surfaces far away from the source is the result of impurity transport through the plasma. Obviously, a large part of the injected droplet material did not reach the core plasma or left it quickly. In TFR-400, material removed from test probes that had been inserted into the scrape-off plasma showed much more pronounced maxima in wall deposition near the probes [12].

Because of the isotropic emission of the macroparticles from the source, the distributions in Fig. 9 are nearly the same in the two toroidal directions. However, comparing the depositions from the two toroidal directions on probe surfaces 180° toroidally away from the source, the collected flux of tantalum ions in the ion drift direction was systematically found to be 20% higher than that in the electron drift direction (co- and counter-direction to the plasma current). This slightly preferred transport of the injected impurity ions was observed for the two directions of the plasma current, parallel and antiparallel to the magnetic field, and can be explained by streaming of the impurity ions with the background plasma ion flow which is induced by the plasma current.

4. SUMMARY

The path of injected matallic droplets showed distinct deflections in the counter-direction to the plasma current. Dust particles released from the wall or limiters showed the same behaviour. It is concluded that these deflections are caused by an asymmetric ablation of the particles which is due to anisotropic heat flux.

The evaporated droplet material was non-uniformly distributed around the torus. The deposition on limiter-like surfaces near the source was about ten times higher than that on surfaces 180° toroidally away from the source.

REFERENCES

[1] ANDERSEN, V., in Controlled Fusion and Plasma Physics (Proc. 12th Eur. Conf. Budapest, 1985), Vol. 9F, Part II, European Physical Society (1985) 648.
[2] McCRACKEN, G.M., STOTT, P.E., Nucl. Fusion **19** (1979) 889.
[3] HILDEBRANDT, D., JÜTTNER, B., JAKUBKA, K., STÖCKEL, J., ZACEK, F., Contrib. Plasma Phys. **27** (1987) 455.
[4] HILDEBRANDT, D., JÜTTNER, B., PURSCH, H., JAKUBKA, K., STÖCKEL, J., ZACEK, F., Studies of Impurity Injection into a Tokamak Plasma, ZIE-Preprint 87–4, Central Institute of Electron Physics, Berlin (1987).
[5] DAALDER, J.E., Physica C **104** (1981) 91.
[6] LINS, G., IEEE Trans. Plasma Sci. **PS-15** (1987) 552.
[7] DISATNIK, G., BOXMANN, R.L., GOLDSMITH, S., IEEE Trans. Plasma Sci. **PS-15** (1987) 520.
[8] OHKAWA, T., Dust Particles as a Possible Source of Impurities in Tokamaks, Rep. GA-A-14232, General Atomics, San Diego, CA (1976).
[9] ECKSTEIN, W., VERBEEK, H., in Data Compendium for Plasma–Surface Interactions, Special Issue 1984, Nucl. Fusion (1984) 12.
[10] ANDERSEN, H.H., BAY, H.L., in Sputtering by Particle Bombardment I (BEHRISCH, R., Ed.), Springer-Verlag, Heidelberg (1981).
[11] GOODALL, D.H.J., CONLON, T.W., SOFIELD, C., McCRACKEN, G.M., J. Nucl. Mater. **76/77** (1978) 492.
[12] BEHRISCH, R., BLEWER, R.S., KUKRAL, H., et al., J. Nucl. Mater. **76/77** (1978) 437.

(Manuscript received 1 August 1988
Final manuscript received 10 November 1988)